

# THE INVERSE FAST MULTIPOLE METHOD

SIVARAM AMBIKASARAN\* AND ERIC DARVE†

An  $\mathcal{O}(N)$  fast direct solver.

**Abstract.** This article introduces a new fast direct solver for linear systems arising out of wide range of applications, integral equations, multivariate statistics, radial basis interpolation, etc., to name a few. *The highlight of this new fast direct solver is that the solver scales linearly in the number of unknowns in all dimensions.* The solver, termed as Inverse Fast Multipole Method (abbreviated as IFMM), works on the same data-structure as the Fast Multipole Method (abbreviated as FMM). More generally, the solver can be immediately extended to the class of hierarchical matrices, denoted as  $\mathcal{H}^2$  matrices with strong admissibility criteria (weak low-rank structure), i.e., *the interaction between neighboring cluster of particles is full-rank whereas the interaction between particles corresponding to well-separated clusters can be efficiently represented as a low-rank matrix.* The algorithm departs from existing approaches in the fact that throughout the algorithm the interaction corresponding to neighboring clusters are always treated as full-rank interactions. Our approach relies on two major ideas: (i) The  $N \times N$  matrix arising out of FMM (from now on termed as FMM matrix) can be represented as an extended sparser matrix of size  $M \times M$ , where  $M \approx 3N$ . (ii) While solving the larger extended sparser matrix, *the fill-in's that arise in the matrix blocks corresponding to well-separated clusters are hierarchically compressed.* The ordering of the equations and the unknowns in the extended sparser matrix is strongly related to the local and multipole coefficients in the FMM [33] and *the order of elimination is different from the usual nested dissection approach.* Numerical benchmarks on 2D manifold confirm the linear scaling of the algorithm.

**Key words.** Fast direct solvers, Hierarchical matrices,  $\mathcal{H}^2$ , Fast Multipole Method, Sparse matrices, Low-rank matrices, Extended sparsification, Hierarchical compression

**1. Introduction.** Large dense matrices arising out of many applications such as integral equations, interpolation, inverse problems, etc., can be efficiently represented as hierarchical matrices, which are data sparse representations of certain class of dense matrices. Detailed discussions on different hierarchical matrix structures can be found in [15–17, 21, 22, 31, 37–41, 43, 44]. The FMM enables computing fast matrix vector products for a sub-class of these hierarchical matrices, i.e., obtaining  $b = Ax$ , where the matrix  $A$  is a FMM matrix at a computational cost of  $\mathcal{O}(N)$ , given a tolerance  $\epsilon$ . In this article, we provide an algorithm to answer the opposite question:

“Can we construct a direct solver for the linear system  $Ax = b$ , given the right hand side  $b$  and a specified error tolerance  $\epsilon$ , where  $A$  is a FMM matrix at a computational cost of  $\mathcal{O}(N)$ ?”

Traditionally, solving linear systems of the form  $Ax = b$ , where  $A$  is a FMM matrix has been done using iterative solver. However, in recent times, there has been an increasing focus on constructing fast direct solvers for these hierarchical matrices [3, 8, 21, 22, 35, 47, 48, 52, 53]. This endeavor has been fruitful in the case of hierarchical matrices with weak-admissibility criteria (strong low-rank structure), i.e., the interaction between non-overlapping regions is represented as a low-rank interaction. This includes the HODLR [3, 8, 48] and HSS matrices [21, 22, 47, 53]. However, the weak admissibility criteria (strong low-rank structure) is restrictive. The rank of the non-overlapping clusters is more or less constant for problems arising out of 1D manifolds but is no longer valid for singular Green’s function of elliptic PDE’s on 2D and 3D manifolds, i.e., the rank of interaction between neighboring clusters is no longer independent of  $N$ . For instance, the rank grows as  $\mathcal{O}(\sqrt{N})$  on 2D manifolds and grows as  $\mathcal{O}(N^{2/3})$  on 3D manifolds. Hence, the scaling of existing fast direct solvers is no longer linear in higher dimensions. This article addresses this issue by constructing a fast direct solver, which relies only on compressing the interaction corresponding to non-neighboring clusters. More precisely, the article presents a new fast direct solver for solving linear systems of the form  $K\sigma = \phi$ , where  $K \in \mathbb{R}^{N \times N}$  is an FMM matrix, in  $\mathcal{O}(N)$  operations with a controllable error  $\epsilon$ . The algorithm also extends to the more general class of matrices known as  $\mathcal{H}^2$  matrices (hierarchical matrices with nested basis) with strong admissibility criteria (weak low-rank structure).

Below are the class of problems that the solver proposed in this article is capable of solving.

1. **Integral equations:** Integral equations arising from elliptic partial differential equations are of the

\*Courant Institute of Mathematical Sciences, New York University, New York, NY 10012

†Institute for Computational and Mathematical Engineering, Huang Engineering Center, Via Ortega, Stanford University, Stanford, CA 94305-4042

form:

$$a(\vec{x})\sigma(\vec{x}) + \int_{\Omega} b(\vec{x})G(\|\vec{x} - \vec{y}\|) c(\vec{y})\sigma(\vec{y})d\vec{y} = \phi(\vec{x}) \quad (1.1)$$

where  $\vec{x} \in \mathbb{R}^n$ ,  $\sigma(\vec{x}) \in \mathbb{R}^n \mapsto \mathbb{R}$  is the unknown function and  $a(\vec{x}), b(\vec{x}), c(\vec{x}), \phi(\vec{x}) : \mathbb{R}^n \mapsto \mathbb{R}$  are known functions. The function  $G(r)$  is the Green's function of the underlying elliptic partial differential equation. Table 1.1 lists some examples of different Green's functions.

Elliptic PDE	Green's function
Laplace/Poisson in 2D	$\log(r)$
Laplace/Poisson in 3D	$1/r$
Helmholtz in 2D	$H_0^{(1)}(kr)$
Helmholtz in 3D	$\frac{\exp(-ikr)}{r}$

TABLE 1.1  
Examples of Green's function  $G(r)$

Discretizing (1.1) leads us to solving a system of the form:

$$K\sigma = \phi$$

where  $\phi \in \mathbb{R}^N$  is known,  $\sigma \in \mathbb{R}^N$  is unknown and the matrix  $K \in \mathbb{R}^{N \times N}$  possesses a FMM structure [49].

**Remark 1.** In case of Helmholtz's, and in general any oscillatory Green's function, the solver is applicable for only moderately high frequency problems.

- Dense covariance matrices:** Dense covariance matrices [6, 59] arising in many applications in inverse problems [5], Kalman filtering [50, 51], statistics, machine learning, Gaussian process [4, 7], etc., can be efficiently represented as FMM matrices [5]. The entries of the covariance matrix,  $K \in \mathbb{R}^{N \times N}$ , arise from the covariance functions,  $C(r)$ , i.e.,  $K(i, j) = C(\|\vec{x}_i - \vec{x}_j\|)$ . Table 1.2 lists some examples of different choices of the covariance functions,  $C(r)$ .

Ornstein Uhlenbeck/ Exponential	$\exp(-r/a)$
Squared exponential/ Gaussian	$\exp(-r^2/a)$
Rational quadratic	$\frac{1}{(1+r^2)^\alpha}$
Matérn	$\frac{(\sqrt{2\nu r}/\rho)^\nu}{\Gamma(\nu)2^{\nu-1}} K_\nu(\sqrt{2\nu r}/\rho)$

TABLE 1.2  
Examples of covariance functions  $C(r)$

- Radial basis function interpolation:** Radial basis function interpolation for multivariate approximation is one of the most frequently applied techniques in approximation theory to represent scattered data in multiple dimensions. The literature on interpolation using radial basis function is vast and we refer the reader to a few [14, 18, 27, 60, 62, 64]. Table 1.3 lists the commonly used radial basis functions and the corresponding matrices, i.e.,  $K(i, j) = R(\|\vec{x}_i - \vec{x}_j\|)$  can be well-represented as FMM matrices [3, 13, 19, 36].

**Remark 2.** In addition to the radial basis functions in Table 1.3, the covariance functions in Table 1.2 are also used in radial basis function interpolation.

The rest of the article is organized as follows. Section 2 sets the background for the rest of the article, by introducing linear solvers, low-rank matrices and the different hierarchical structures. The next section,

Multi-quadric	$(1 + r^2/a^2)^{1/2}$
Inverse multi-quadric	$(1 + r^2/a^2)^{-1/2}$
Poly-harmonic spline I	$r^{2k+1}$
Poly-harmonic spline II	$r^{2k} \log(r)$

TABLE 1.3  
List of radial basis functions  $R(r)$

Section 3 presents the key ideas, discusses some previous work on fast direct solvers and highlights the contributions of the present work. A comprehensive discussion on how our approach differs from existing ones is highlighted. Section 4 discusses the extended sparsification & hierarchical compression algorithm, which is followed by the section on numerical benchmark.

## 2. Background.

**2.1. Iterative versus direct solvers.** Algorithms for solving linear systems can be broadly classified into: (i) Iterative solvers (ii) Direct solvers. Most of the iterative solvers are based on Krylov subspace techniques [9, 29, 30, 46, 55, 58, 61] and rely on matrix-vector products. The number of iterations required to achieve a target accuracy is highly problem dependent. In many instances, the large condition number of the matrix or distribution of the eigenvalues of the matrix in the complex plane (e.g., widely spread eigenvalues) result in a large number of iterations. Consequently, pre-conditioners need to be devised to cluster the eigenvalues and thereby accelerate convergence of the iterative solver. Once such a pre-conditioner is in place, the cost of performing the matrix-vector products can be reduced using fast summation techniques like the fast multipole method (FMM) [12, 24, 54], the Barnes-Hut algorithm [10], panel clustering [42], FFT, wavelet based methods, and others. Of these different fast summation techniques, FMM has often been used in the context of linear systems arising out of boundary integral equations. This is because the Green's function resulting from such integral equations are amenable to FMM [11, 23, 25, 26, 28, 32–34, 65]. With these in place, fast iterative solvers solve the linear system in linear or almost linear complexity.

Direct solvers on the other hand rely on efficient factorization/elimination —Gaussian elimination/LU, QR, etc. —of the underlying linear system and then using the factorization to obtain the solution. Direct solvers possess a wide range of advantages: (i) The solution can be computed exactly (up-to machine precision), (ii) Scales well with multiple right hand sides (iii) Robust and hence preferred for black-box implementations. However, the major draw back of direct solvers is that it is highly expensive, since the factorization/elimination step scales as  $\mathcal{O}(N^3)$  for most of the dense matrices. The focus of this article is to reduce the computational complexity of direct solvers to  $\mathcal{O}(N)$  for the class of FMM matrices.

**2.2. FMM matrices /  $\mathcal{H}^2$  matrices with strong admissibility (weak low-rank structure).** For readers familiar with FMM [33],  $\mathcal{H}^2$  matrices are an algebraic version of the matrices encountered in the FMM. A minor difference is that in the FMM, the geometric domain is hierarchically partitioned using a  $2^d$  tree in  $d$  dimensions. But in the case of  $\mathcal{H}^2$  matrices, the tree is not restricted to a  $2^d$  tree in  $d$  dimensions. Table 2.2, Figure 2.2 and Figure 2.3 illustrate the FMM matrices, on 1D and 2D manifolds at different levels in the tree.

**Remark 3.** Note that Figure 2.2 and Figure 2.3 do not explicitly reveal the nested low-rank structure. The low-rank basis at the parent level is constructed from the low-rank basis of its children.

In general, based on the admissibility and nested low-rank structure, hierarchical matrices are classified as shown in Table 2.1 and Figure 2.1. For a detailed description of these different hierarchical structures, we refer the readers to Chapter 3 of [2]. The fast direct solver algorithm presented in the article also extends to other hierarchical structures, though that will not be the focus of the current article. Refer Chapter 7 of [2], where the algorithm is discussed for HSS and HODLR matrices.

**3. Key ideas, previous work and contribution of this article.** There are couple of novel ideas exploited in this article to attain linear complexity.

- The first key idea is that one form of sparsity can be converted into another form of sparsity, which can then be exploited. To be specific, a  $N \times N$  data-sparse FMM matrix can exactly be represented as a  $M \times M$  extended structured sparse matrix, where  $M \in \mathcal{O}(N)$ . The unknowns of the original dense linear system are a subset of the unknowns of the extended sparse linear system. (We use the

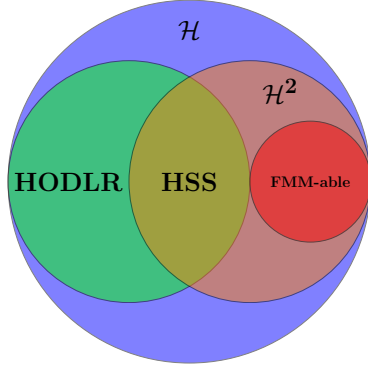


FIG. 2.1. An Euler diagram of the different hierarchical matrices

		Nested basis	
		No	Yes
Low-rank structure	Strong	HODLR	HSS
	Weak	$\mathcal{H}$	$\mathcal{H}^2$

TABLE 2.1  
Different hierarchical structures.

$$K^{(2)} = \begin{bmatrix} K_{11}^{(2)} & K_{12}^{(2)} & U_1^{(2)} \tilde{K}_{13}^{(2)} V_3^{(2)T} & U_1^{(2)} \tilde{K}_{14}^{(2)} V_4^{(2)T} \\ K_{21}^{(2)} & K_{22}^{(2)} & K_{23}^{(2)} & U_2^{(2)} \tilde{K}_{24}^{(2)} V_4^{(2)T} \\ U_3^{(2)} \tilde{K}_{31}^{(2)} V_1^{(2)T} & K_{32}^{(2)} & K_{33}^{(2)} & K_{34}^{(2)} \\ U_4^{(2)} \tilde{K}_{41}^{(2)} V_1^{(2)T} & U_4^{(2)} \tilde{K}_{42}^{(2)} V_2^{(2)T} & K_{43}^{(2)} & K_{44}^{(2)} \end{bmatrix}$$

TABLE 2.2

A 2 level FMM matrix based on a binary tree, where the points lie on an interval with the natural ordering in 1D. The matrices  $\tilde{K}_{ij}^{(2)}$ ,  $U_i^{(2)}$ ,  $V_j^{(2)}$  are low-rank matrices.

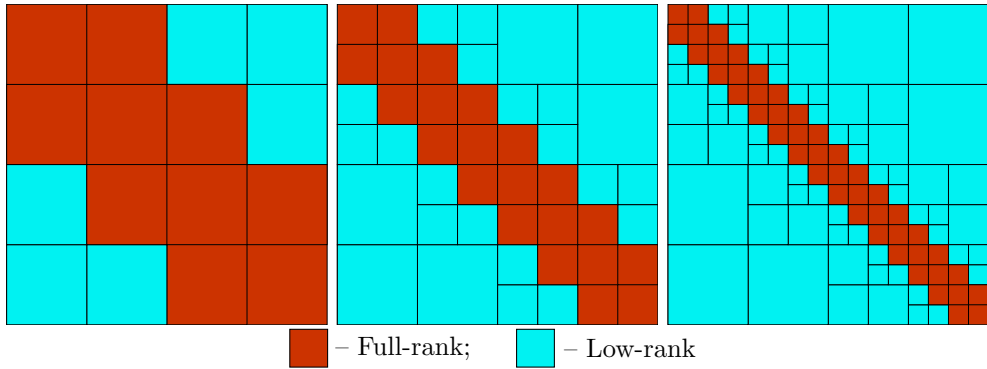


FIG. 2.2. The figure shows the FMM matrix based on a binary tree, where the points lie on an interval with the natural ordering in 1D. Left: Level 2; Middle: Level 3; Right: Level 4. The figures do not reveal the nested low-rank structure. The row and column basis of the low-rank matrices at a level in the tree can be constructed from the row and column basis of the low-rank matrices of its children.

term sparse matrix in the conventional sense; i.e., a matrix primarily populated with zeros. This should not be confused with data-sparsity, i.e., a matrix with low-rank sub-blocks.)

- The second *key ingredient* is that, when performing the elimination of unknowns in the extended sparse linear system, the interaction between the unknowns corresponding to the well-separated clusters at all stages in the elimination process can be efficiently compressed as low-rank, which is validated in Tables 3.1 and 3.2 for different kernel functions.

This implies, after an appropriate ordering of equations and unknowns, while we perform the elimination, the fill-in that occurs in the elimination process corresponding to well-separated clusters can be compressed and efficiently represented as a low-rank matrix. As shown in Section 4, the ordering of the equations and the unknowns in the extended sparser matrix is strongly related to the local and multipole coefficients in the fast multipole method, which is different from the one obtained

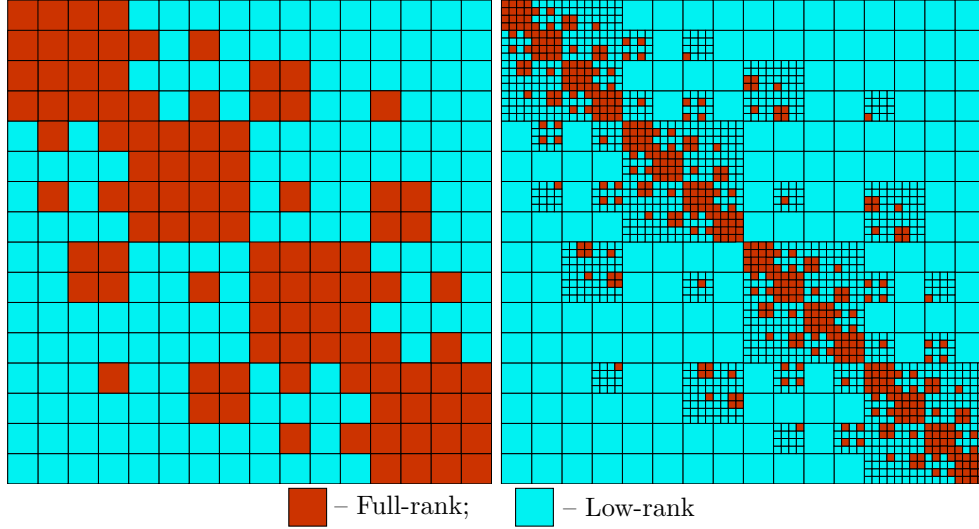


FIG. 2.3. The figure shows the FMM matrix based on a quad tree, where the points lie on a 2D manifold homeomorphic to a square with Morton ordering/ Z-ordering. Left: Level 2; Right: Level 3. The figure on the right does not reveal the nested low-rank structure present in the matrix. The row and column basis of the low-rank matrices at level 2 in the tree can be constructed from the row and column basis of the low-rank matrices of its children at level 3.

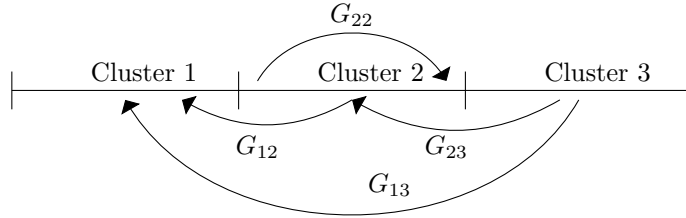


FIG. 3.1. The relevant interactions along a 1D manifold for Table 3.1.  $N$  denotes the number of particles in each cluster.

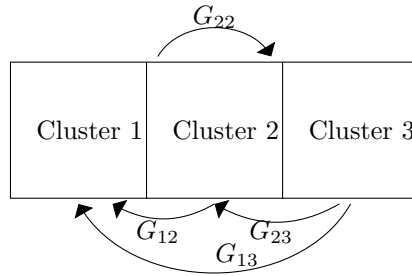


FIG. 3.2. The relevant interactions along a 2D manifold for Table 3.2.  $N$  denotes the number of particles in each cluster.

using the nested dissection approach.

Before discussing our algorithm, we present a brief discussion of previous works in this direction and our new contribution. The idea of extended sparsification has been considered before in the article by Chandrasekaran et al. [22], though only in the context of HSS matrices, which are strict sub-class of  $\mathcal{H}^2$  matrices, i.e., has the additional constraint that the interaction between all (not just the “well-separated clusters”) are low-rank. The algorithm for HSS matrices is fairly easier since in the elimination process there are *no new fill-ins*. However, hierarchically semi-separable matrices are restricted to one-dimensional applications. In our approach, we deal with the larger class of FMM matrices, which model a large class of hierarchical matrices in all dimensions.

Kernels	$N$	Neighbor rank	Well-separated rank	
			Interaction	Schur complement
		$G_{12}$	$G_{13}$	$G_{13} - G_{12}G_{22}^{-1}G_{23}$
Logarithm $\left(\frac{r(\log(r) - 1)}{a(\log(a) - 1)}\right) \chi_{r < a} + \left(\frac{\log(r)}{\log(a)}\right) \chi_{t \geq a}$	32	14	9	8
	64	16	9	9
	128	18	9	9
	256	19	8	8
	512	21	8	8
	1024	24	8	8
	2048	28	8	8
Bessel function of second kind $\left(\frac{1 + y_0(a)}{1 + y_0(r)}\right) \chi_{r < a} + \left(\frac{y_0(r)}{y_0(a)}\right) \chi_{r \geq a}$	32	14	10	9
	64	16	10	9
	128	18	9	9
	256	20	9	9
	512	22	9	9
	1024	24	9	9
	2048	29	9	9
Inverse quadric $\left(\frac{\arctan(r)}{\arctan(a)}\right) \chi_{r < a} + \left(\frac{1 + a^2}{1 + r^2}\right) \chi_{r \geq a}$	32	14	9	9
	64	15	9	8
	128	14	9	9
	256	14	9	9
	512	15	9	8
	1024	18	9	8
	2048	23	9	7
Inverse multi-quadric $\left(\frac{\operatorname{arcsinh}(r)}{\operatorname{arcsinh}(a)}\right) \chi_{r < a} + \left(\sqrt{\frac{1 + a^2}{1 + r^2}}\right) \chi_{r \geq a}$	32	14	9	8
	64	15	9	9
	128	15	9	9
	256	14	8	8
	512	14	8	8
	1024	17	8	8
	2048	22	8	8

TABLE 3.1

Ranks of different interactions in 1D to a precision of  $10^{-15}$ , i.e.,  $\frac{\sigma_{r+1}}{\sigma_1} < 10^{-15}$ , where  $r$  is the rank and  $\sigma_i$  are the singular values.  $a$  was taken as 0.005 of the length of the interval.

Further it is non trivial to extend the algorithm presented in Chandrasekaran et al. [22] to FMM matrices. To achieve linear complexity for FMM matrices, *it is to be emphasized that the second step mentioned in Section 3 is highly crucial*. For instance, Pals, in his thesis [56], follows a similar approach of representing the matrix arising out of fast multipole method as an extended sparser matrix, but does not exploit the fact that the fill-ins can be compressed as we proceed through the algorithm. Instead Pals [56] rely on nested dissection using METIS to solve the sparse linear system and show that even though the extended sparser approach is faster, the scaling of the algorithm is still in fact very close to  $\mathcal{O}(N^3)$  (Refer Chapter 4 of [56]). This is due to the fact that the conventional nested dissection approach doesn't exploit the fact that the fill-ins are low-rank.

Greengard et al. [35] present the idea of representing the dense matrix as an extended sparse matrix. The article presents a single-level fast solver whose scaling is not  $\mathcal{O}(N)$  and due to which compressing the fill-ins, which is important to extend the strategy in a multi-level setting, is not discussed.

Ho and Greengard [47] discuss the use of extended sparsification technique mentioned in [21], i.e., based on HSS representations and a recursive skeletonization approach, in the context of integral equations, where the compression is obtained using the interpolative decomposition technique. The computational complexity scales like  $\mathcal{O}(N)$  on 1D manifolds.

Ambikasaran's thesis [2] discusses the  $\mathcal{O}(N)$  extended sparsification technique for HSS matrices and extends it to the bigger class of HODLR matrices at a computational complexity of  $\mathcal{O}(N \log^2 N)$ , with

Kernels	$N$	Neighbor rank	Well-separated rank	
			Interaction	Schur complement
		$G_{12}$	$G_{13}$	$G_{13} - G_{12}G_{22}^{-1}G_{23}$
Logarithm $\left(\frac{r(\log(r)-1)}{a(\log(a)-1)}\right)\chi_{r<a} + \left(\frac{\log(r)}{\log(a)}\right)\chi_{t\geq a}$	64	26	18	17
	121	31	19	19
	225	33	19	19
	441	37	19	21
	841	41	19	22
	1681	44	18	23
	3249	46	18	24
Bessel function of second kind $\left(\frac{1+y_0(a)}{1+y_0(R)}\right)\chi_{r<a} + \left(\frac{y_0(R)}{y_0(a)}\right)\chi_{t\geq a}$	64	28	21	19
	121	33	21	23
	225	37	22	23
	441	40	22	25
	841	44	22	26
	1681	47	21	27
	3249	49	22	28
3D Laplace $\left(\frac{r}{a}\right)\chi_{r<a} + \left(\frac{a}{r}\right)\chi_{r\geq a}$	64	53	36	38
	121	68	38	42
	225	78	39	45
	441	88	38	43
	841	94	39	45
	1681	103	37	45
	3249	110	37	45
3D Helmholtz $\left(\frac{r}{a}\right)\chi_{r<a} + \left(\frac{a\cos(r)}{r\cos(a)}\right)\chi_{r\geq a}$	64	56	43	45
	121	73	44	42
	225	82	45	50
	441	93	45	52
	841	101	45	50
	1681	108	45	47
	3249	116	43	51
Biharmonic $\left(\frac{r^3(3\log(r)-1)}{a^3(3\log(a)-1)}\right)\chi_{r<a} + \left(\frac{r^2\log(r)}{a^2\log(a)}\right)\chi_{r\geq a}$	64	38	25	21
	121	43	25	20
	225	49	27	20
	441	52	26	20
	841	57	27	20
	1681	58	25	20
	3249	62	25	20

TABLE 3.2

Ranks of different interactions in 2D to a precision of  $10^{-15}$ , i.e.,  $\frac{\sigma_{r+1}}{\sigma_1} < 10^{-15}$ , where  $r$  is the rank and  $\sigma_i$  are the singular values.  $a$  was taken as 0.005 of the length of the side of the square.

application to interpolation using radial basis functions.

There have also been other attempts not based on the extended sparsification technique. Broadly speaking, these techniques rely on factorizing the matrix instead of introducing additional variables and we refer the readers to the work by Hackbusch and coworkers [38, 40, 41]. Ambikasaran & Darve [3] and Kong et al. [48] discuss an  $\mathcal{O}(N \log^2 N)$  algorithm on 1D manifolds in the context of radial basis function interpolation and integral equations respectively using HODLR matrices. The algorithm is based on the Sherman-Morrison-Woodbury formula [45, 63]. Ambikasaran & Darve [3] also extend the algorithm to the context of HSS matrices at a computational complexity of  $\mathcal{O}(N \log N)$ .

A  $ULV^T$  decomposition ( $U$  and  $V$  are unitary matrices, and  $L$  is lower triangular) of a HSS matrix is discussed in work by Chandrasekaran et al. [22]. The key ingredient of their algorithm is to recognize that with a low-rank approximation of the form  $UBV^H$ , it is possible to apply a unitary transformation to have

the last set of rows of  $U$  to be non-zero. This is then applied recursively in a “bottom-up” fashion to attain the factorization at a computational complexity of  $\mathcal{O}(N)$ .

The work by Rokhlin and Martinsson [53] constructs an  $\mathcal{O}(N)$  fast direct solver for boundary integral equations in two-dimensions (i.e., one dimensional manifold) making use of off-diagonal low-rank blocks, i.e., a HSS representation of the matrix. The algorithm constructs the inverse using a compressed block factorization that takes advantage of the low-rank off-diagonal blocks to factor the matrix.

To summarize, most of the previous work on fast direct solvers [3, 20–22, 47, 48, 53] rely on HSS approach. The main drawback of the HSS based fast direct solver is that it is restrictive, especially for applications involving dense matrices arising in 2D and 3D. In particular, the rank of the off-diagonal blocks grow as  $\mathcal{O}(N^{1/2})$  and  $\mathcal{O}(N^{2/3})$  in 2D and 3D respectively.

The main contribution of the algorithm discussed in this paper is that we abandon the HSS matrix framework and work with the more general class of FMM matrices throughout the algorithm. There has been some previous work on  $\mathcal{H}^2$  matrices [15, 16, 39], but they are mainly restricted to almost linear complexity matrix-vector products and fast iterative solvers. To our knowledge, this is the first direct solver for FMM matrices in all dimensions. It is to be noted that Börm [15] discusses an algorithm for  $\mathcal{H}^2$  matrix-matrix multiplications. Using this a fast direct solver for  $\mathcal{H}^2$  matrices could be constructed but the pre-factor tends to be large, since the  $\mathcal{H}^2$  matrix-matrix multiplications are expensive, despite their linear complexity. The numerical benchmarks of our algorithm indicate that the pre-factor in the scaling is not that large and large problems can be solved in a reasonable amount of time.

**Remark 4.** *The most important aspect of the algorithm discussed in this article is that **at all stages** in the algorithm, we only represent the interaction between well-separated clusters as “low-rank”, i.e., we only rely on compressing the interaction between “well-separated” clusters. Hence, the “low-rank” matrices considered in our algorithm are “truly” low-rank, i.e., the rank of these matrices is independent of  $N$ , the cluster size.*

**4. Fast direct solver for FMM matrices.** In this section, we first look at how the dense FMM matrix can be interpreted as an extended sparser matrix. It is worth recalling that in the FMM tree data structure in  $d$  dimensions, we have a  $2^d$  tree and there are local and multipole coefficients at each level in the tree. To form the extended sparser system, we introduce these local and multipole coefficients as unknowns, and the corresponding set of relations between them as equations. *We then present a new ordering of the equations/relations, which is different from the nested dissection ordering for sparse linear systems.*

**Remark 5.** *We first choose to explain the algorithm in 1D and using pictures of matrices and their corresponding graphs. This is done for a couple of reasons.*

- *Explaining in 1D succinctly captures almost all the key features of the algorithm (Refer remark 7).*
- *Pictures of matrices and their graphs provides an easy way to internalize the algorithm.*

*The general algorithm applicable in any dimension is presented later in section 4.2.*

**4.1. Illustration in 1D.** Consider the linear equation (4.1) obtained from a 2 level FMM matrix on an interval in 1D.

#### 4.1.1. Ordering of equations and unknowns.

$$\begin{bmatrix} K_{11}^{(2)} & K_{12}^{(2)} & U_1^{(2)} \tilde{K}_{13}^{(2)} V_3^{(2)T} & U_1^{(2)} \tilde{K}_{14}^{(2)} V_4^{(2)T} \\ K_{21}^{(2)} & K_{22}^{(2)} & K_{23}^{(2)} & U_2^{(2)} \tilde{K}_{24}^{(2)} V_4^{(2)T} \\ U_3^{(2)} \tilde{K}_{31}^{(2)} V_1^{(2)T} & K_{32}^{(2)} & K_{33}^{(2)} & K_{34}^{(2)} \\ U_4^{(2)} \tilde{K}_{41}^{(2)} V_1^{(2)T} & U_4^{(2)} \tilde{K}_{42}^{(2)} V_2^{(2)T} & K_{43}^{(2)} & K_{44}^{(2)} \end{bmatrix} \begin{bmatrix} x_1^{(2)} \\ x_2^{(2)} \\ x_3^{(2)} \\ x_4^{(2)} \end{bmatrix} = \begin{bmatrix} b_1^{(2)} \\ b_2^{(2)} \\ b_3^{(2)} \\ b_4^{(2)} \end{bmatrix} \quad (4.1)$$

Let us now introduce the multipoles and locals for each cluster. The multipoles and locals for each cluster are given in Equation (4.2) and Equation (4.3).

$$y_1^{(2)} = V_1^{(2)T} x_1; y_2^{(2)} = V_2^{(2)T} x_2; y_3^{(2)} = V_3^{(2)T} x_3; y_4^{(2)} = V_4^{(2)T} x_4 \quad (4.2)$$

$$z_1^{(2)} = \tilde{K}_{13}^{(2)} y_3^{(2)} + \tilde{K}_{14}^{(2)} y_4^{(2)}; z_2^{(2)} = \tilde{K}_{24}^{(2)} y_4^{(2)}; z_3^{(2)} = \tilde{K}_{31}^{(2)} y_1^{(2)}; z_4^{(2)} = \tilde{K}_{41}^{(2)} y_1^{(2)} + \tilde{K}_{42}^{(2)} y_2^{(2)} \quad (4.3)$$

Introducing Equations (4.2) & (4.3) in Equation (4.1), gives us Equation (4.4).

$$\begin{bmatrix}
 K_{11}^{(2)} & K_{12}^{(2)} & 0 & 0 & U_1^{(2)} & 0 & 0 & 0 & 0 & 0 & 0 & 0 \\
 K_{21}^{(2)} & K_{22}^{(2)} & K_{23}^{(2)} & 0 & 0 & U_2^{(2)} & 0 & 0 & 0 & 0 & 0 & 0 \\
 0 & K_{32}^{(2)} & K_{33}^{(2)} & K_{34}^{(2)} & 0 & 0 & U_3^{(2)} & 0 & 0 & 0 & 0 & 0 \\
 0 & 0 & K_{43}^{(2)} & K_{44}^{(2)} & 0 & 0 & 0 & U_4^{(2)} & 0 & 0 & 0 & 0 \\
 0 & 0 & 0 & 0 & -I & 0 & 0 & 0 & 0 & 0 & \tilde{K}_{13}^{(2)} & \tilde{K}_{14}^{(2)} \\
 0 & 0 & 0 & 0 & 0 & -I & 0 & 0 & 0 & 0 & 0 & \tilde{K}_{24}^{(2)} \\
 0 & 0 & 0 & 0 & 0 & 0 & -I & 0 & \tilde{K}_{31}^{(2)} & 0 & 0 & 0 \\
 0 & 0 & 0 & 0 & 0 & 0 & 0 & -I & \tilde{K}_{41}^{(2)} & \tilde{K}_{42}^{(2)} & 0 & 0 \\
 V_1^{(2)T} & 0 & 0 & 0 & 0 & 0 & 0 & 0 & -I & 0 & 0 & 0 \\
 0 & V_2^{(2)T} & 0 & 0 & 0 & 0 & 0 & 0 & 0 & -I & 0 & 0 \\
 0 & 0 & V_3^{(2)T} & 0 & 0 & 0 & 0 & 0 & 0 & 0 & -I & 0 \\
 0 & 0 & 0 & V_4^{(2)T} & 0 & 0 & 0 & 0 & 0 & 0 & 0 & -I
 \end{bmatrix}
 \begin{bmatrix}
 x_1^{(2)} \\
 x_2^{(2)} \\
 x_3^{(2)} \\
 x_4^{(2)} \\
 z_1^{(2)} \\
 z_2^{(2)} \\
 z_3^{(2)} \\
 z_4^{(2)} \\
 y_1^{(2)} \\
 y_2^{(2)} \\
 y_3^{(2)} \\
 y_4^{(2)}
 \end{bmatrix}
 =
 \begin{bmatrix}
 b_1^{(2)} \\
 b_2^{(2)} \\
 b_3^{(2)} \\
 b_4^{(2)} \\
 0 \\
 0 \\
 0 \\
 0 \\
 0 \\
 0 \\
 0 \\
 0
 \end{bmatrix}
 \quad (4.4)$$

Note that with the default ordering of equations and unknowns the matrix in Equation (4.4) is asymmetric in terms of fill-in. We now reorder the equations and unknowns to make the matrix into a symmetric matrix as shown in Equation (4.5).

$$\begin{bmatrix}
 K_{11}^{(2)} & U_1^{(2)} & K_{12}^{(2)} & 0 & 0 & 0 & 0 & 0 & 0 & 0 & 0 & 0 \\
 V_1^{(2)T} & 0 & 0 & 0 & 0 & 0 & 0 & 0 & -I & 0 & 0 & 0 \\
 K_{21}^{(2)} & 0 & K_{22}^{(2)} & U_2^{(2)} & K_{23}^{(2)} & 0 & 0 & 0 & 0 & 0 & 0 & 0 \\
 0 & 0 & V_2^{(2)T} & 0 & 0 & 0 & 0 & 0 & 0 & -I & 0 & 0 \\
 0 & 0 & K_{32}^{(2)} & 0 & K_{33}^{(2)} & U_3^{(2)} & K_{34}^{(2)} & 0 & 0 & 0 & 0 & 0 \\
 0 & 0 & 0 & 0 & V_3^{(2)T} & 0 & 0 & 0 & 0 & 0 & -I & 0 \\
 0 & 0 & 0 & 0 & K_{43}^{(2)} & 0 & K_{44}^{(2)} & U_4^{(2)} & 0 & 0 & 0 & 0 \\
 0 & 0 & 0 & 0 & 0 & 0 & V_4^{(2)T} & 0 & 0 & 0 & 0 & -I \\
 0 & -I & 0 & 0 & 0 & 0 & 0 & 0 & 0 & 0 & \tilde{K}_{13}^{(2)} & \tilde{K}_{14}^{(2)} \\
 0 & 0 & 0 & -I & 0 & 0 & 0 & 0 & 0 & 0 & 0 & \tilde{K}_{24}^{(2)} \\
 0 & 0 & 0 & 0 & 0 & -I & 0 & 0 & \tilde{K}_{31}^{(2)} & 0 & 0 & 0 \\
 0 & 0 & 0 & 0 & 0 & 0 & 0 & -I & \tilde{K}_{41}^{(2)} & \tilde{K}_{42}^{(2)} & 0 & 0
 \end{bmatrix}
 \begin{bmatrix}
 x_1^{(2)} \\
 z_1^{(2)} \\
 x_2^{(2)} \\
 z_2^{(2)} \\
 x_3^{(2)} \\
 z_3^{(2)} \\
 x_4^{(2)} \\
 z_4^{(2)} \\
 y_1^{(2)} \\
 y_2^{(2)} \\
 y_3^{(2)} \\
 y_4^{(2)}
 \end{bmatrix}
 =
 \begin{bmatrix}
 b_1^{(2)} \\
 0 \\
 b_2^{(2)} \\
 0 \\
 b_3^{(2)} \\
 0 \\
 b_4^{(2)} \\
 0 \\
 0 \\
 0 \\
 0 \\
 0
 \end{bmatrix}
 \quad (4.5)$$

The extended sparse matrix in the above equation is pictorially represented as shown in Figure 4.1. The

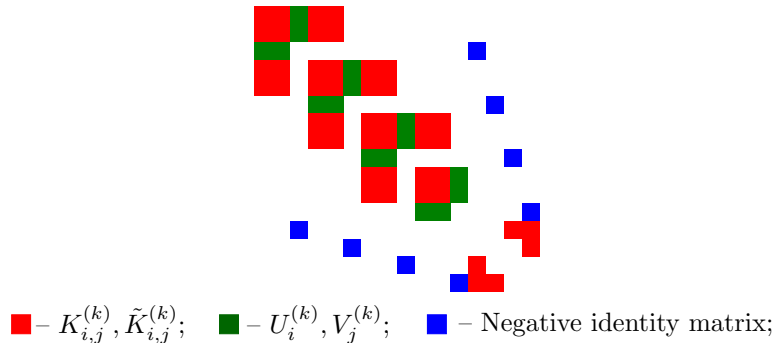


FIG. 4.1. Sparsity pattern of FMM matrix at level 3 arising out of a 1D manifold homeomorphic to an interval represented as an extended sparse matrix after appropriate ordering of equations and unknowns.

color code as shown in Figure 4.1 will be followed in the rest of the article as well; Red in the extended sparse matrix denotes the matrices  $K_{i,j}^{(k)}$  &  $\tilde{K}_{i,j}^{(k)}$ , i.e., the direct interactions and M2L operators; Dark green

denotes the interpolation/scatter/L2L/L2P operator & the antepolation/gather/M2M/P2M operator; Blue denotes the negative identity matrix.

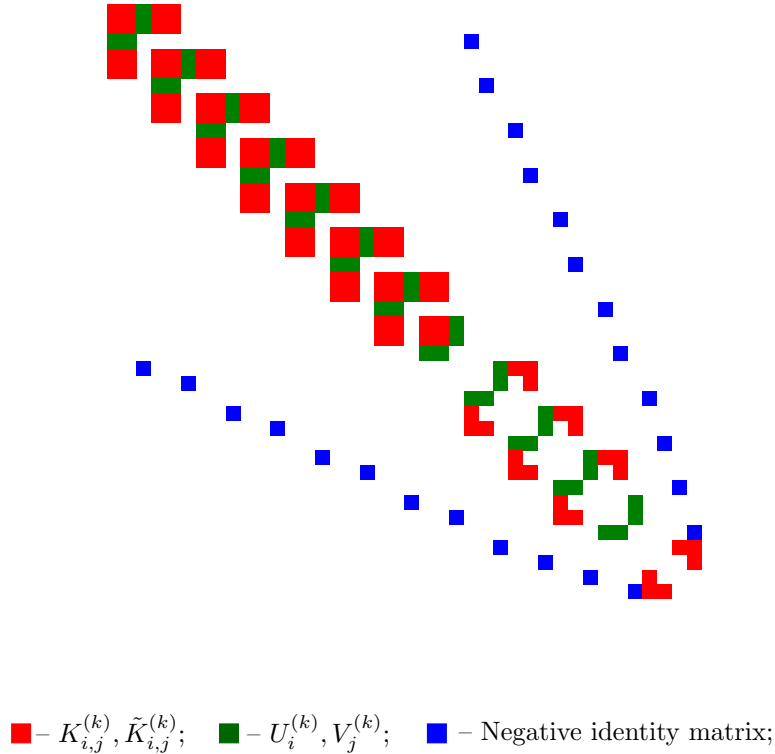


FIG. 4.2. Sparsity pattern of FMM matrix at level 3 arising out of a 1D manifold homeomorphic to an interval represented as an extended sparse matrix after appropriate ordering of equations and unknowns.

**4.1.2. Elimination and hierarchical compression.** Before we describe the algorithm, we would like to mention a key fact.

**Remark 6.** It is important to note that if we feed in the sparse matrix in Figure 4.2 to a conventional sparse matrix solver, **we will not obtain an  $\mathcal{O}(N)$  algorithm**. This is because there will be fill-in's, which is detrimental to the linear scaling. For instance, if we eliminate the set of rows and columns corresponding to the leaf level without any compression, the matrix we obtain has a complete fill-in as shown in Figure 4.3(a). For the linear scaling, what we need is that the matrix pattern after eliminating the rows and columns of leaf, should look like Figure 4.1. The fill-ins are detrimental to the scaling of the algorithm. In our algorithm, these fill-ins are compressed since these correspond to interaction between well-separated clusters. Let us see how this is done by viewing the appropriate graph of this extended sparse-matrix.

Figures 4.4– 4.13 explain the first few steps of the algorithm in 1D.

**Remark 7.** In 2D and 3D, eliminating a cluster will also result in P2P fill-in. If this P2P fill-in corresponds to an interaction between well-separated clusters, this needs to be compressed as well. On an interval in 1D, eliminating under the natural ordering results in no P2P fill-in. However, if we were to eliminate in order other than the natural ordering, there will be a P2P fill-in, which needs to be compressed.

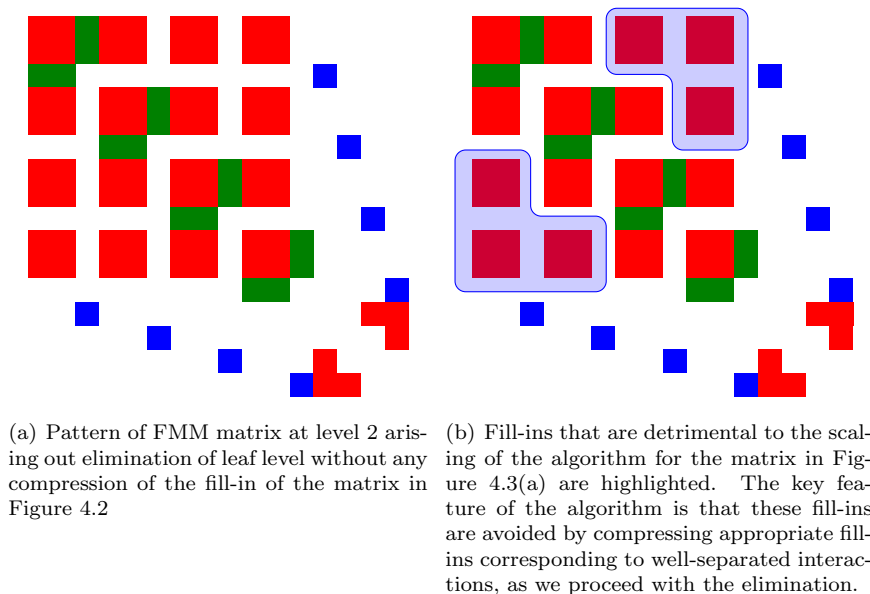


FIG. 4.3. Extended sparse matrix at level 2 after eliminating the nodes of the matrix in Figure 4.2 corresponding to level 3.

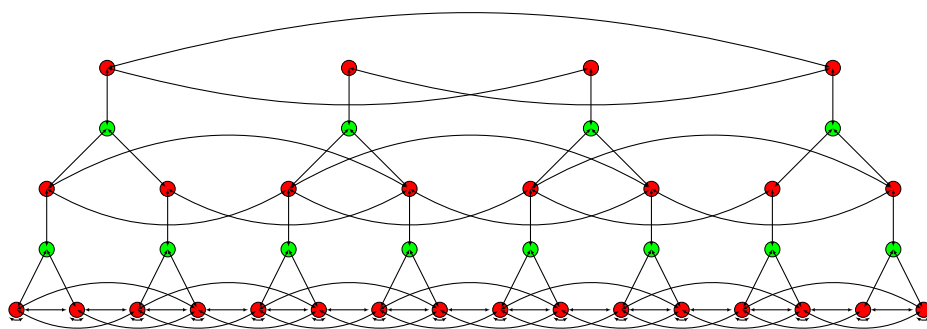


FIG. 4.4. The graph of the 3 level extended sparse matrix in Figure 4.2. The leaf consists of the bottom 16 red nodes and the 8 green nodes connected to them.

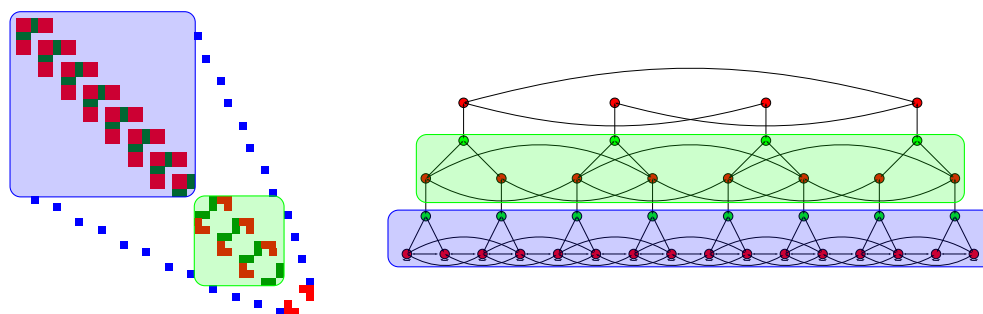


FIG. 4.5. The duality between corresponding blocks of the matrix and the nodes & edges of the graph at the leaf level are highlighted.

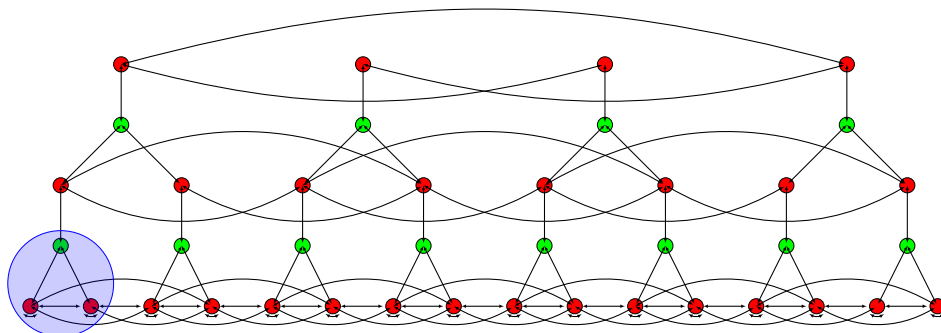


FIG. 4.6. *Preparing to eliminate the particles and the corresponding local coefficients at the leaf level for the first set of clusters at the leaf level.*

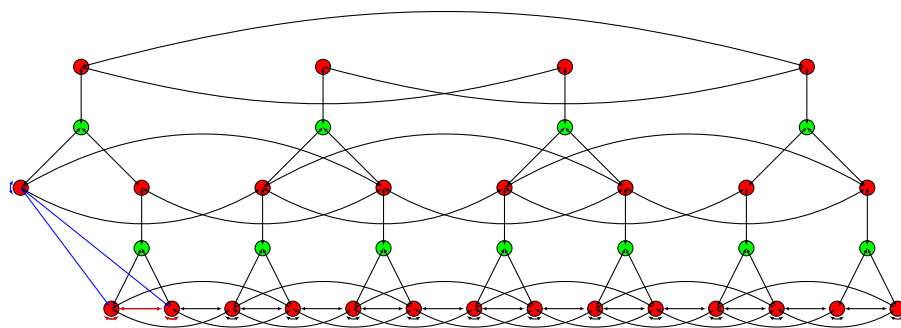


FIG. 4.7. *Eliminating the first set of clusters in the previous step results in a fill-in (the edges corresponding to the fill-in are shown in blue color) between multipoles of the cluster with itself and with the particles of the neighbor. This also updates the interaction between the particles of the neighbors (the updated edges are shown in red color).*

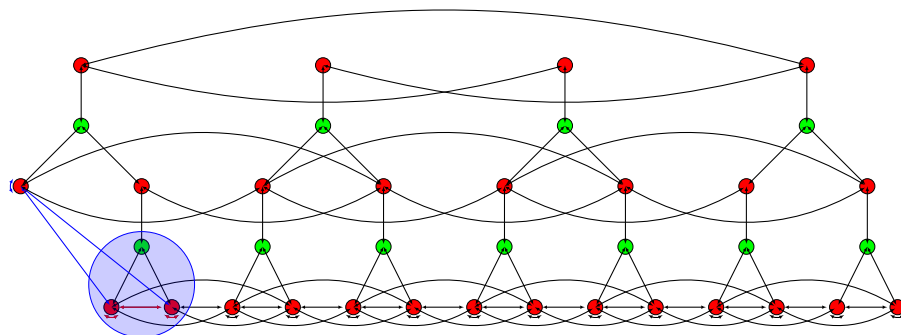


FIG. 4.8. *Preparing to eliminate the next set of particles and the local coefficients of the second set of clusters at the leaf level.*

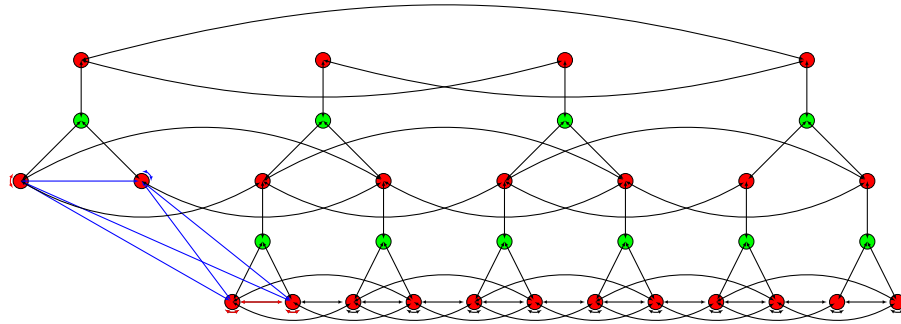


FIG. 4.9. Eliminating the second set of clusters result in fill-in between the multipoles of the first, multipoles of the second cluster and the particles of the third cluster, in addition to a fill-in in the multipoles of the second cluster with itself. Further, this also updates the interaction of the first set of multipoles with itself and the interaction of the particles of the third cluster with itself.

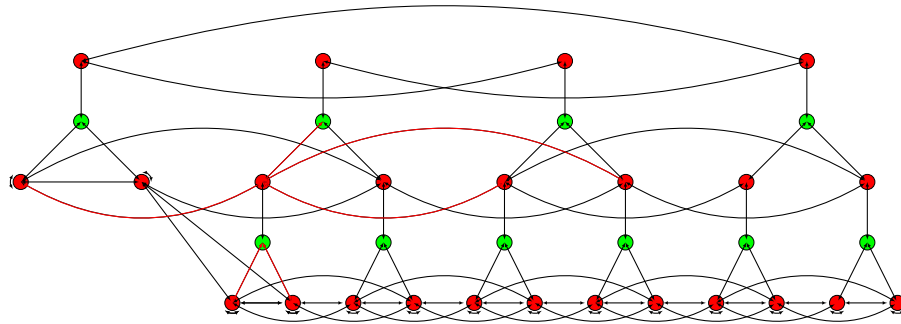


FIG. 4.10. This step is the key step since this reduces the fill-ins as we proceed with the elimination. As we saw in the previous step (Figure 4.9), the fill-in appears between the multipoles of the first set of clusters and the particles of the third set of clusters. This fill-in corresponds to a well-separated interaction. This fill-in is compressed along with the L2L/M2M basis of the third cluster, i.e., the interaction between the multipoles of the first cluster and the particles of the third cluster is redirected through the multipoles and local of the third cluster. This results in updating the following operators of the second cluster: (a) the M2L operator capturing the interaction with its interaction list, (b) the P2M and L2P operators, (c) the P2M and L2P operator of its parent.

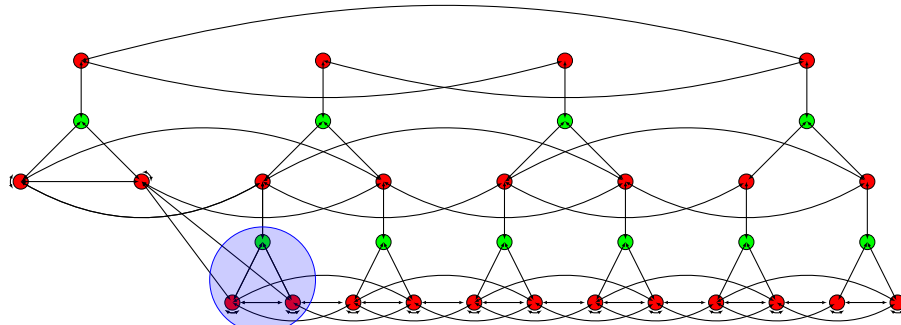


FIG. 4.11. Preparing to eliminate the third set of particles and their local coefficients at the leaf level.

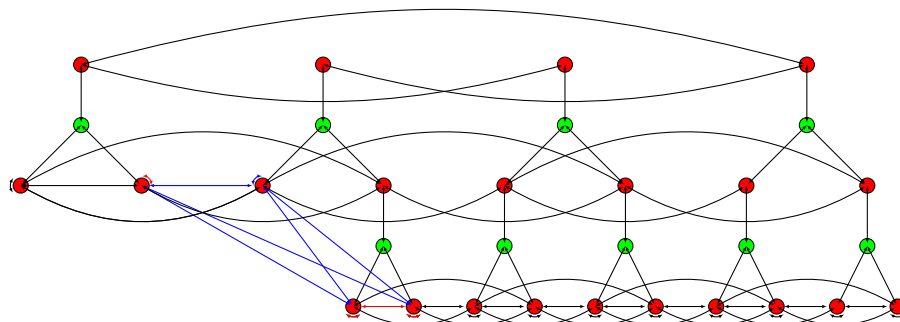


FIG. 4.12. Eliminating the third set of clusters result in fill-in between the multipoles of the second, multipoles of the third cluster and the particles of the fourth cluster, in addition to a fill-in in the multipoles of the third cluster with itself. Further, this also updates the interaction of the second set of multipoles with itself and the interaction of the particles of the fourth cluster with itself.

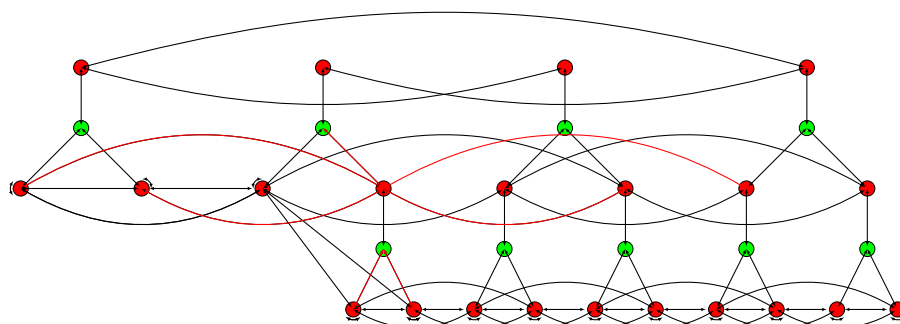


FIG. 4.13. This step reduces the fill-ins as we proceed with the elimination. As we saw in the previous step (Figure 4.12), the fill-in appears between the multipoles of the second set of clusters and the particles of the fourth set of clusters. This fill-in corresponds to a well-separated interaction. This fill-in is compressed along with the L2L/M2M basis of the fourth cluster, i.e., the interaction between the multipoles of the second cluster and the particles of the fourth cluster is redirected through the multipoles and local of the fourth cluster. This results in updating the following operators of the fourth cluster: (a) the M2L operator capturing the interaction with its interaction list, (b) the P2M and L2P operators, (c) the P2M and L2P operator of its parent.

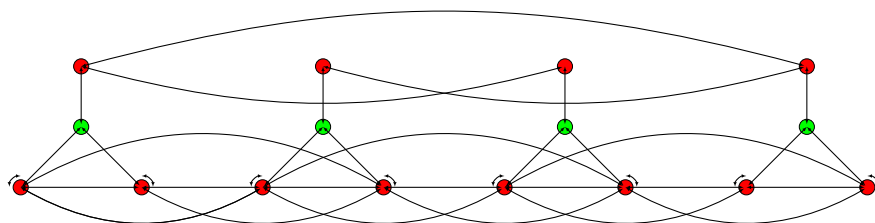


FIG. 4.14. Repeat this for all clusters at the leaf level (in our case the third level). Now repeat the process for the all the clusters at the second level by interpreting the multipoles of the leaf level as particles at this level. And proceed level by level. Once the elimination phase is done, we need to do the back substitution phase, which proceeds exactly in the reverse order.

**4.2. General algorithm.** In general, in any dimension, set up the FMM tree, i.e., sub-divide the domain using a  $2^d$  tree in  $d$  dimensions. We will work with a non-adaptive/uniform tree for pedagogical reasons. At each level of the tree, we have unknown particles, multipoles and locals. We first introduce some notations in Table 4.1 to denote different clusters.

$\mathcal{C}_i^{(k)}$	Cluster $i$ at level $k$ .
$\mathcal{N}_i^{(k)}$	Neighbors of $\mathcal{C}_i^{(k)}$ including self.
$\mathcal{I}_i^{(k)}$	Interaction list, i.e., well-separated clusters that are children of parents neighbors.

TABLE 4.1  
*Different lists associated with cluster 'i' at level 'k'*

Each cluster  $\mathcal{C}_i^{(k)}$  has the variables shown in Table 4.2.

$x_i^{(k)}$	Unknown charges on particles
$y_i^{(k)}$	Unknown multipole coefficients
$z_i^{(k)}$	Unknown local coefficients
$r_i^{(k)}$	Known right hand side or the potential
$E_i^{(k)}$	1 if the cluster is eliminated; 0 otherwise

TABLE 4.2  
*Known and unknown variables associated with cluster 'i' at level 'k'*

Note that by particles at a non-leaf level, we mean the multipoles of its children, i.e.,

$$x_i^{(k)} = \left[ y_{i_1}^{(k+1)} \quad y_{i_2}^{(k+1)} \quad \dots \quad y_{i_{2^d}}^{(k+1)} \right]^T \quad (4.6)$$

where  $i_p$  is a child of cluster  $i$ . As for the right hand side, the right hand side at each of the non-leaf level is set as zero, while the right hand side for each cluster at the leaf level is the input right hand side, i.e., the potential at these points. Refer Equation (4.5) as to why this should be the case. The local coefficients  $z_i^{(k)}$  is the potential on the multipoles due to well-separated clusters. Note that  $z_i^{(1)} = 0$ , since there is no well-separated cluster at the first level in the tree.

Table 4.3 presents the operators needed for the FMM. In case of the FMM,  $P2P_{ij}^{(k)}$  is non-zero only for  $\mathcal{C}_i^{(k)} \in \mathcal{N}_j^{(k)}$  and  $M2L_{ij}^{(k)}$  is non-zero for  $\mathcal{C}_i^{(k)} \in \mathcal{I}_j^{(k)}$ .

$P2P_{ij}^{(k)}$	Potential on particles in $\mathcal{C}_i^{(k)}$ due to charges in $\mathcal{C}_j^{(k)}$ .
$P2M_{ii}^{(k)}$	Lumping the charges in $\mathcal{C}_i^{(k)}$ to its multipoles.
$L2P_{ii}^{(k)}$	Interpolating the potential from locals in $\mathcal{C}_i^{(k)}$ to its particles.
$M2L_{ij}^{(k)}$	Potential on locals of $\mathcal{C}_i^{(k)}$ due to the multipoles of $\mathcal{C}_j^{(k)}$ .

TABLE 4.3  
*Different interaction operators associated with cluster 'i' at level 'k'*

For the IFMM, there will be a fill-in in  $P2P_{ij}^{(k)}$ , where  $\mathcal{C}_i^{(k)} \in \mathcal{I}_j^{(k)}$ , though this will be compressed on the fly. Apart from this, we need two additional operators for the IFMM as shown in Table 4.4.

$P2L_{ij}^{(k)}$	Local potentials in $\mathcal{C}_i^{(k)}$ due to charges in $\mathcal{C}_j^{(k)}$ .
$M2P_{ij}^{(k)}$	Potential on particles in $\mathcal{C}_i^{(k)}$ due to multipoles in $\mathcal{C}_j^{(k)}$ .

TABLE 4.4  
*Different interaction operators associated with cluster 'i' at level 'k'*

The  $P2L_{ij}^{(k)}$  and  $M2P_{ij}^{(k)}$  operators are needed only if  $\mathcal{C}_i^{(k)} \in \mathcal{N}_j^{(k)} \cup \mathcal{I}_j^{(k)}$  and will be zero to begin with. However, while performing elimination these operators will get populated. The  $P2L_{ij}^{(k)}$  and  $M2P_{ij}^{(k)}$  operators for  $\mathcal{C}_i^{(k)} \in \mathcal{I}_j^{(k)}$  will be compressed on the fly as well, i.e., for well-separated clusters

- $P2L_{ij}^{(k)}$  will be expressed using the  $M2L_{ij}^{(k)}$  and  $P2M_{jj}^{(k)}$  by beefing up the “multipoles” of  $\mathcal{C}_j^{(k)}$ .
- $M2P_{ij}^{(k)}$  will be expressed using the  $L2P_{ii}^{(k)}$  and  $M2L_{ij}^{(k)}$  by beefing up the “locals” of  $\mathcal{C}_i^{(k)}$ .

**Remark 8.** *P2P operator at non-leaf levels is initially zero. As we proceed with the elimination, the P2P operator will be defined using the M2L operator of its children, i.e.,*

$$P2P_{ij}^{(k)} = \begin{bmatrix} M2L_{i_1 j_1}^{(k+1)} & M2L_{i_1 j_2}^{(k+1)} & M2L_{i_1 j_3}^{(k+1)} & \dots & M2L_{i_1 j_{2d}}^{(k+1)} \\ M2L_{i_2 j_1}^{(k+1)} & M2L_{i_2 j_2}^{(k+1)} & M2L_{i_2 j_3}^{(k+1)} & \dots & M2L_{i_2 j_{2d}}^{(k+1)} \\ M2L_{i_3 j_1}^{(k+1)} & M2L_{i_3 j_2}^{(k+1)} & M2L_{i_3 j_3}^{(k+1)} & \dots & M2L_{i_3 j_{2d}}^{(k+1)} \\ \vdots & \vdots & \vdots & \ddots & \vdots \\ M2L_{i_{2d} j_1}^{(k+1)} & M2L_{i_{2d} j_2}^{(k+1)} & M2L_{i_{2d} j_3}^{(k+1)} & \dots & M2L_{i_{2d} j_{2d}}^{(k+1)} \end{bmatrix}$$

where  $i_p$  is a child of cluster  $i$  and  $j_q$  is a child of cluster  $j$ .

**Remark 9.** *Note that the M2L between two clusters at level  $k+1$ , i.e., the interaction between multipoles and locals of these two clusters, forms part of a neighbor interaction — a particle particle interaction — at level  $k$ .*

**Remark 10.** *At the beginning of the algorithm, i.e., once the FMM data structure has been set up, the following are zero:*

- $P2L_{ij}^{(k)}, M2P_{ij}^{(k)}$ ;
- $M2L_{ij}^{(k)}$ , where  $j \in \mathcal{N}_i^{(k)}$ ;
- $P2P_{ij}^{(k)}$  and  $r_i^{(k)}$  at the non-leaf levels;
- $E_j^{(k)} = 0$ .

**4.2.1. Overall idea of the algorithm.** Let  $\kappa$  be the number of levels in the tree, i.e., the level  $\kappa$  consists of leaves. Let  $n_k$  denote the number of clusters at level  $k$ . For our purposes, we have  $n_k = 2^k$ . Below is a short snippet of the overall idea.

• **Elimination phase/ Upward pass**

- Eliminate cluster by cluster at the lowest level. Elimination order at level  $k$ :  $\{e_1^{(k)}, e_2^{(k)}, \dots, e_{n_k}^{(k)}\}$ .
- Eliminating cluster, say  $e_i^{(k)}$ , results in fill-in among all its neighboring clusters, i.e., if  $j_1, j_2 \in \mathcal{N}_i^{(k)}$ , we then have a
  - \*  $P2P_{j_1, j_2}^{(k)}$  and  $P2P_{j_2, j_1}^{(k)}$  fill-in if  $j_1, j_2$  have not been yet eliminated.
  - \*  $P2L_{j_1, j_2}^{(k)}$  and  $M2P_{j_2, j_1}^{(k)}$  fill-in if  $j_1$  has been eliminated and  $j_2$  has not been yet eliminated.
  - \*  $M2L_{j_1, j_2}^{(k)}$  and  $M2L_{j_2, j_1}^{(k)}$  fill-in if  $j_1, j_2$  have been eliminated.
- Fill-ins between well-separated clusters, i.e.,  $P2P, P2L, M2P$  are compressed and directed through the appropriate  $P2M, M2L, L2P$  operators, thereby eliminating the fill-ins.
- Repeat this at all levels marching up the tree, till we are left just with the particles at level 1.
- Solve for these particles at level 1, which are nothing but the multipoles at level 2.

• **Back substitution phase/ Downward pass**

- Back-substitute for each cluster starting from level 2 marching downward in the tree.
- Back substitution order at level ‘ $k$ ’ is the reverse of the elimination order at level ‘ $k$ ’, i.e.,  $\{e_{n_k}^{(k)}, e_{n_k}^{(k-1)}, \dots, e_2^{(k)}, e_1^{(k)}\}$

**4.2.2. Main algorithm in all dimensions.** The algorithm has an upward pass and a downward pass. The upward pass begins with clusters at the leaf level  $\kappa$  and proceeds up till level 1, while the downward pass begins with clusters at level 1 and proceeds all the way till level  $\kappa$ . While performing the upward pass at level  $k$ , there are two main equations,  $P2P(i, k)$  and  $P2M(i, k)$ , to be considered for cluster  $i$  at this level.

- **P2P equation:** Equation (4.7) will be denoted as P2P(i,k).

$$\underbrace{P2P_{ii}^{(k)} x_i^{(k)}}_{\text{Direct self}} + \underbrace{L2P_{ii}^{(k)} z_i^{(k)}}_{\text{L2L self}} + \sum_{j \in \mathcal{N}_i^{(k)}} \left( \underbrace{P2P_{ij}^{(k)} x_j^{(k)} (1 - E_j^{(k)})}_{\text{Direct neighbor}} + \underbrace{M2P_{ij}^{(k)} y_j^{(k)} E_j^{(k)}}_{\text{Multipoles of neighbors}} \right) = \begin{bmatrix} r_{i_1}^{(k+1)} \\ r_{i_2}^{(k+1)} \\ \dots \\ r_{i_{2d}}^{(k+1)} \end{bmatrix} \quad (4.7)$$

- **P2M equation:** Equation (4.8) will be denoted as P2M(i,k).

$$P2M_{ii}^{(k)} x_i^{(k)} - y_i^{(k)} = 0 \quad (4.8)$$

The elimination phase (upward pass) is presented in Algorithm 1, while Algorithm 2 presents the back-substitution phase (downward pass). Note that the elimination phase involves more work (compressing the fill-ins) than the back-substitution phase. It is also important to note that, as with any direct solver, the “factorization phase” (in our case most of the elimination phase), can be decoupled from the “solve phase” (back-substitution phase) making it attractive for multiple right hand-sides.

**Algorithm 1:** Elimination phase/ Upward pass**Input:** The FMM tree**Output:** Eliminates all the cluster

```

1 for  $k = \kappa, \kappa - 1, \dots, 2$  do
2   for  $i = e_1^{(k)}, e_2^{(k)}, \dots, e_{n_k}^{(k)}$  do
3     Form  $P2P$  operator for cluster  $i$  with its neighbors from  $M2L$  operators of its children;
4   for  $i = e_1^{(k)}, e_2^{(k)}, \dots, e_{n_k}^{(k)}$  do
5     Eliminate  $x_i^{(k)}$  and  $z_i^{(k)}$  using the equations  $P2P(i,k)$  and  $P2M(i,k)$ ;
6     Set  $E_i^{(k)} = 1$ ;
7     This results in the following fill-ins among neighbors of  $i$ ;
8     Consider the pair  $(p, q)$ , where  $C_p^{(k)}, C_q^{(k)} \in \mathcal{N}_i^{(k)}$ ;
9     if  $p$  has been eliminated then
10      if  $q$  has been eliminated then
11        Results in updating the  $M2L_{pq}^{(k)}$  and  $M2L_{qp}^{(k)}$  operator;
12      else if  $q$  has not been eliminated then
13        Results in  $P2L_{pq}^{(k)}$  and  $M2P_{qp}^{(k)}$  fill-in;
14        if  $p$  and  $q$  are well-separated then
15          Compress  $P2L_{pq}^{(k)}$ , i.e.,  $P2L_{pq}^{(k)} = M2L_{pq}^{(k)} P2M_{qq}^{(k)}$ ;
16          Compress  $M2P_{qp}^{(k)}$ , i.e.,  $M2P_{qp}^{(k)} = L2P_{qq}^{(k)} M2L_{qp}^{(k)}$ ;
17          Update the following operators:
          •  $P2M_{qq}^{(k)}, L2P_{qq}^{(k)}, M2L_{lq}^{(k)}, M2L_{ql}^{(k)}$  operators, where  $l \in \mathcal{N}_q^{(k)} \cup \mathcal{I}_q^{(k)}$ ;
          •  $P2M_{q'q'}, L2P_{q'q'}$ , where  $q'$  is the parent of  $q$ ;
18      else if  $p$  has not been eliminated then
19        if  $q$  has been eliminated then
20          Results in  $P2L_{qp}^{(k)}$  and  $M2P_{pq}^{(k)}$  fill-in;
21          if  $p$  and  $q$  are well-separated then
22            Compress  $P2L_{qp}^{(k)}$ , i.e.,  $P2L_{qp}^{(k)} = M2L_{qp}^{(k)} P2M_{pp}^{(k)}$ ;
23            Compress  $M2P_{pq}^{(k)}$ , i.e.,  $M2P_{pq}^{(k)} = L2P_{pp}^{(k)} M2L_{pq}^{(k)}$ ;
24            Update the following operators:
            •  $P2M_{pp}^{(k)}, L2P_{pp}^{(k)}, M2L_{lp}^{(k)}, M2L_{pl}^{(k)}$  operators, where  $l \in \mathcal{N}_p^{(k)} \cup \mathcal{I}_p^{(k)}$ ;
            •  $P2M_{p'p'}, L2P_{p'p'}$ , where  $p'$  is the parent of  $p$ ;
25          else if  $q$  has not been eliminated then
26            Results in  $P2P_{pq}^{(k)}$  and  $P2P_{qp}^{(k)}$  fill-in;
27            if  $p$  and  $q$  are well-separated then
28              Compress  $P2P_{pq}^{(k)}$ , i.e.,  $P2P_{pq}^{(k)} = L2P_{pp}^{(k)} M2L_{pq}^{(k)} P2M_{qq}^{(k)}$ ;
29              Compress  $P2P_{qp}^{(k)}$ , i.e.,  $P2P_{qp}^{(k)} = L2P_{qq}^{(k)} M2L_{qp}^{(k)} P2M_{pp}^{(k)}$ ;
30              Update the following operators:
              •  $L2P_{pp}^{(k)}, P2M_{pp}^{(k)}, L2P_{qq}^{(k)}, P2M_{qq}^{(k)}$ ;
              •  $M2L_{lp}^{(k)}, M2L_{pl}^{(k)}$  operators, where  $l \in \mathcal{N}_p^{(k)} \cup \mathcal{I}_p^{(k)}$ ;
              •  $M2L_{lq}^{(k)}, M2L_{ql}^{(k)}$  operators, where  $l \in \mathcal{N}_q^{(k)} \cup \mathcal{I}_q^{(k)}$ ;
              •  $P2M_{p'p'}, L2P_{p'p'}$ , where  $p'$  is the parent of  $p$ ;
              •  $P2M_{q'q'}, L2P_{q'q'}$ , where  $q'$  is the parent of  $q$ ;

```

**Algorithm 2:** Back-Substitution phase/ Downward pass**Input:** Eliminated tree**Output:** Back-Substituted tree

---

```

1 for  $k = 1, 2, \dots, \kappa$  do
2   for  $i = e_{n_k}^{(k)}, e_{n_k-1}^{(k)}, \dots, e_2^{(k)}, e_1^{(k)}$  do
3     Obtain  $x_i^{(k)}$  and  $z_i^{(k)}$  using equation P2P(i,k) and P2M(i,k);
4     Set  $E_i^{(k)} = 0$ ;
5     Get  $y_{i_1}^{(k+1)}, y_{i_2}^{(k+1)}, \dots, y_{i_{2d}}^{(k+1)}$  from  $x_i^{(k)}$  using Equation (4.6).

```

---

**5. Numerical benchmarks.** We present numerical benchmarks of the algorithm on a 2D manifold for the following equation

$$\sigma_i + \sum_{\substack{j=1 \\ j \neq i}}^{j=N} K(\vec{r}_i, \vec{r}_j) \sigma_j = f_i, \quad \forall i \in \{1, 2, \dots, N\} \quad (5.1)$$

on three different singular kernels;

- (i)  $\left(\frac{r(\log(r) - 1)}{a(\log(a) - 1)}\right) \chi_{r < a} + \left(\frac{\ln(r)}{\ln(a)}\right) \chi_{r \geq a}$
- (ii)  $\left(\frac{r}{a}\right) \chi_{r < a} + \left(\frac{a}{r}\right) \chi_{r \geq a}$
- (iii)  $\left(\frac{r^3(3\log(r) - 1)}{a^3(3\log(a) - 1)}\right) \chi_{r < a} + \left(\frac{r^2 \ln(r)}{a^2 \ln(a)}\right) \chi_{r \geq a}$

We also provide comparison of the new solver with the HODLR fast direct solver discussed in [3], which is available here [1] and also with the conventional full pivoted LU direct solver in Eigen. The algorithm was implemented in C++ and all the tests were run on 2.1GHz with 256GB memory. For each of the benchmark, we follow the conventions shown in Table 5.1.

$N$	Number of unknowns
$r_m$	Maximum rank of compressed sub-matrices
$t_a$	Time taken to assemble the system
$t_f$	Time taken to factor the system
$t_s$	Time taken to apply the factorization, i.e., to solve the system
Error	A known vector $x_{\text{exact}}$ is taken and the right hand side $b$ is obtained. For this right hand side, the system is solved using the proposed algorithm and the relative error in $\ell_2$ norm is obtained, i.e., $\frac{\ x - x_{\text{exact}}\ _2}{\ x_{\text{exact}}\ _2}$

TABLE 5.1  
Notations used in the results

The points  $\vec{r}_i$  are distributed randomly in the square  $[-1, 1] \times [-1, 1]$  such that the FMM tree is balanced. The nested low-rank decomposition of the well-separated clusters are obtained using Chebyshev interpolation by using 8 Chebyshev nodes along one dimension, i.e., a total of 64 Chebyshev nodes in 2D, followed by SVD compression to further reduce the rank. The compression of the fill-ins is obtained using a tweaked version of the adaptive cross approximation algorithm [57, 66]. The tolerance used to compress all the blocks is  $10^{-14}$ . The parameter  $a$  was taken as 0.001.

**Remark 11.** As seen from all the benchmarks, it is important to note that the rank of the compressed blocks for the IFMM remains independent of  $N$ , whereas for the HODLR solver the rank scales up (roughly like  $\sqrt{N}$ ) with  $N$ .

**Benchmark 1.**  $K(r) = \left(\frac{r(\log(r) - 1)}{a(\log(a) - 1)}\right) \chi_{r < a} + \left(\frac{\ln(r)}{\ln(a)}\right) \chi_{r \geq a}$ .

$N$ (in thousands)	$t_a$ in secs		$t_f$ in secs		$t_s$ in secs		$r_m$		Error	
	IFMM	HODLR	IFMM	HODLR	IFMM	HODLR	IFMM	HODLR	IFMM	HODLR
1	0.02	0.07	0.35	0.09	0.007	0.0023	29	105	$10^{-12}$	$10^{-11}$
2	0.02	0.23	0.71	0.26	0.009	0.0055	31	137	$10^{-13}$	$10^{-11}$
5	0.09	1.24	1.68	1.21	0.026	0.0179	30	206	$10^{-12}$	$10^{-9}$
10	0.12	3.81	3.21	3.57	0.06	0.0467	37	257	$10^{-10}$	$10^{-8}$
20	0.26	12.15	6.78	11.31	0.13	0.1219	36	339	$10^{-11}$	$10^{-8}$
50	0.71	60.73	16.79	50.91	0.32	0.4237	40	485	-	-
100	1.78	208.62	34.93	217.83	0.72	2.3386	44	671	-	-
200	3.43	-	73.87	-	1.54	-	48	-	-	-
500	9.87	-	189.63	-	4.09	-	47	-	-	-
1000	18.79	-	412.48	-	8.87	-	51	-	-	-

TABLE 5.2

$$K(r) = \left( \frac{r(\log(r) - 1)}{a(\log(a) - 1)} \right) \chi_{r < a} + \left( \frac{\ln(r)}{\ln(a)} \right) \chi_{r \geq a}, \text{ where points are distributed in } [-1, 1]^2$$

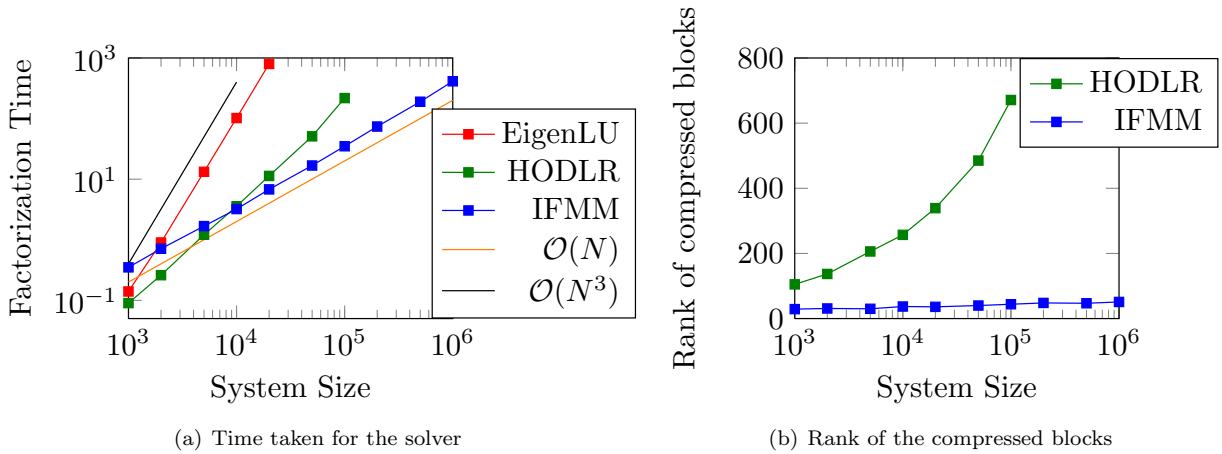


FIG. 5.1.  $K(r) = \left( \frac{r(\log(r) - 1)}{a(\log(a) - 1)} \right) \chi_{r < a} + \left( \frac{\ln(r)}{\ln(a)} \right) \chi_{r \geq a}$ , where points are distributed in  $[-1, 1]^2$

**Benchmark 2.**  $K(r) = \left( \frac{r^3(3 \log(r) - 1)}{a^3(3 \log(a) - 1)} \right) \chi_{r < a} + \left( \frac{r^2 \ln(r)}{a^2 \ln(a)} \right) \chi_{r \geq a}$ .

$N$ (in thousands)	$t_a$ in secs		$t_f$ in secs		$t_s$ in secs		$r_m$		Error	
	IFMM	HODLR	IFMM	HODLR	IFMM	HODLR	IFMM	HODLR	IFMM	HODLR
1	0.01	0.12	0.11	0.15	0.003	0.0029	22	129	$10^{-13}$	$10^{-11}$
2	0.02	0.36	0.27	0.42	0.007	0.0071	21	153	$10^{-12}$	$10^{-10}$
5	0.08	1.73	0.64	1.89	0.017	0.0244	25	222	$10^{-13}$	$10^{-10}$
10	0.14	4.87	1.42	5.47	0.041	0.0684	24	254	$10^{-11}$	$10^{-9}$
20	0.23	15.41	2.76	16.52	0.091	0.1578	27	314	$10^{-12}$	$10^{-8}$
50	0.62	61.21	5.34	68.57	0.262	0.9643	26	411	-	-
100	1.34	166.03	10.89	231.77	0.554	3.5219	28	456	-	-
200	2.59	-	26.47	-	1.192	-	31	-	-	-
500	6.43	-	72.37	-	2.873	-	30	-	-	-
1000	12.12	-	153.93	-	6.121	-	32	-	-	-

TABLE 5.3

$$K(r) = \left( \frac{r^3(3 \log(r) - 1)}{a^3(3 \log(a) - 1)} \right) \chi_{r < a} + \left( \frac{r^2 \ln(r)}{a^2 \ln(a)} \right) \chi_{r \geq a}, \text{ where points are distributed in } [-1, 1]^2$$

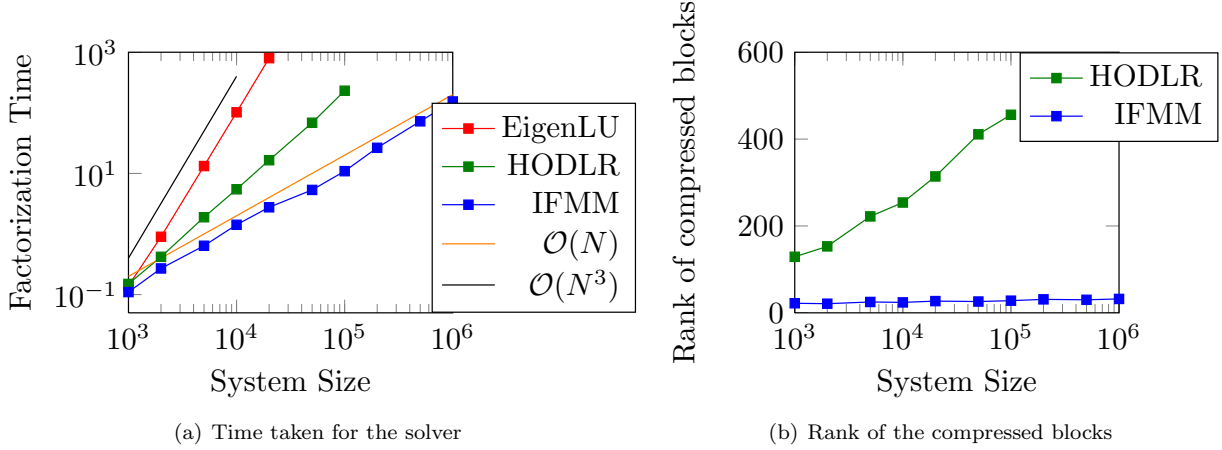


FIG. 5.2.  $K(r) = \left(\frac{r^3(3\log(r)-1)}{a^3(3\log(a)-1)}\right) \chi_{r < a} + \left(\frac{r^2 \ln(r)}{a^2 \ln(a)}\right) \chi_{r \geq a}$ , where points are distributed in  $[-1, 1]^2$

**Benchmark 3.**  $K(r) = \left(\frac{r}{a}\right) \chi_{r < a} + \left(\frac{a}{r}\right) \chi_{r \geq a}$ .

N (in thousands)	$t_a$ in secs		$t_f$ in secs		$t_s$ in secs		$r_m$		Error	
	IFMM	HODLR	IFMM	HODLR	IFMM	HODLR	IFMM	HODLR	IFMM	HODLR
1	0.02	0.22	0.42	0.26	0.005	0.0042	45	141	$10^{-13}$	$10^{-13}$
2	0.05	0.79	1.00	0.62	0.015	0.0102	43	202	$10^{-12}$	$10^{-12}$
5	0.11	4.62	2.37	3.93	0.035	0.0490	49	252	$10^{-13}$	$10^{-13}$
10	0.24	18.93	4.94	16.26	0.092	0.1392	51	363	$10^{-11}$	$10^{-11}$
20	0.51	63.41	9.92	66.02	0.192	0.3478	57	501	$10^{-12}$	$10^{-10}$
50	1.32	332.3	27.39	415.84	0.567	2.0879	54	693	-	-
100	2.73	1269.93	61.34	1712.79	1.213	7.9384	59	998	-	-
200	5.62	-	142.38	-	2.492	-	65	-	-	-
500	14.52	-	398.23	-	5.781	-	68	-	-	-
1000	28.42	-	803.85	-	12.436	-	67	-	-	-

TABLE 5.4  
 $K(r) = \left(\frac{r}{a}\right) \chi_{r < a} + \left(\frac{a}{r}\right) \chi_{r \geq a}$ , where points are distributed in  $[-1, 1]^2$

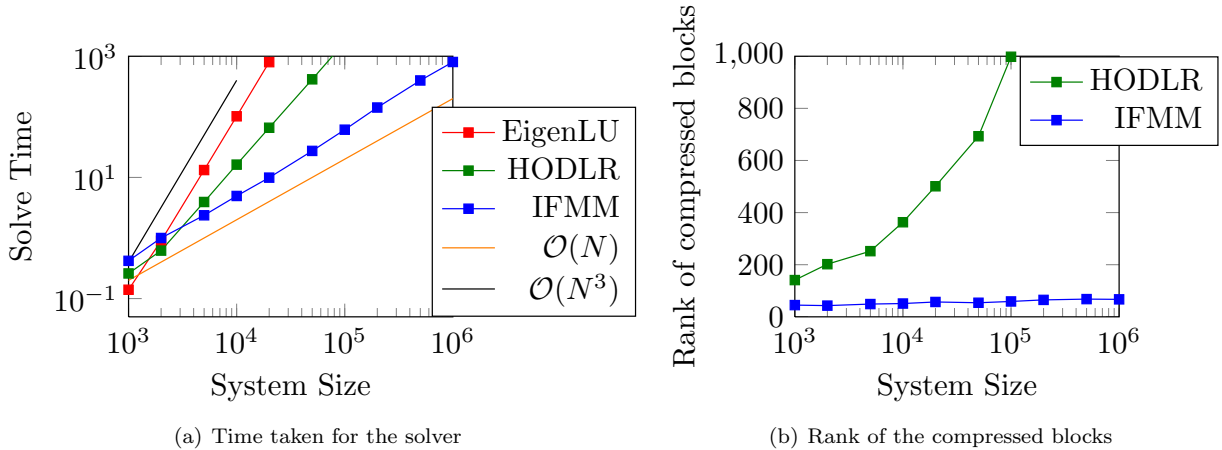


FIG. 5.3.  $K(r) = \begin{pmatrix} r \\ a \end{pmatrix} \chi_{r < a} + \begin{pmatrix} a \\ r \end{pmatrix} \chi_{r \geq a}$ , where points are distributed in  $[-1, 1]^2$

**6. Conclusion.** The article proposes the “Inverse Fast Multipole Method”. The IFMM is a fast direct solver that the solver works on the same data structure as the Fast Multipole Method and relies on compressing only the interactions corresponding to well-separated clusters. The highlight of the solver is that the computational cost scales linearly in the number of unknowns in all dimensions, provided the interactions corresponding to the well-separated clusters at all stages in the algorithm can be efficiently represented as a low-rank matrix. Numerical benchmarks presented validate the  $\mathcal{O}(N)$  scaling of the algorithm for the kernels considered. The IFMM can be extended to integral equations, where the resulting linear system obtained after discretization can be solved at a computational complexity of  $\mathcal{O}(N)$ . It is also important to note that the IFMM can be applied to elliptic PDEs when discretized using local finite difference or fine element methods. In this case, the IFMM will operate on a sparse matrix, which is a special case of a hierarchical matrix with the rank corresponding to well-separated clusters being zero. The algorithm naturally extends itself to  $\mathcal{H}^2$  matrices with strong admissibility criteria (weak low-rank structure).

**7. Acknowledgements.** Sivaram Ambikasaran would like to thank Leslie Greengard and Alex Barnett for helpful discussions in presenting the material. Sivaram Ambikasaran was supported by the Applied Mathematical Sciences Program of the U.S. Department of Energy under Contract DEFGO288ER25053 and by the Office of the Assistant Secretary of Defense for Research and Engineering and AFOSR under NSSEFF Program Award FA9550-10-1-0180. Part of this research was done at Stanford University, and was supported in part by the U.S. Army Research Laboratory, through the Army High Performance Computing Research Center, Cooperative Agreement W911NF-07-0027. This material is also based upon work supported by the Department of Energy National Nuclear Security Administration under Award Number DE-NA0002373-1.

## References.

- [1] Sivaram Ambikasaran. A fast direct solver for dense linear systems. <https://github.com/sivaramambikasaran/HODLR.Solver>, 2013.
- [2] Sivaram Ambikasaran. *Fast Algorithms for Dense Numerical Linear Algebra and Applications*. PhD thesis, Stanford University, 2013.
- [3] Sivaram Ambikasaran and Eric F. Darve. An  $\mathcal{O}(N \log N)$  fast direct solver for partial hierarchically semi-separable matrices. *Journal of Scientific Computing*, 57(3):477–501, 2013.
- [4] Sivaram Ambikasaran and Michael O’Neil. Fast symmetric factorization of hierarchical matrices with applications. *arXiv preprint arXiv:1405.0223*, 2014.
- [5] Sivaram Ambikasaran, Judith Y. Li, Peter K. Kitanidis, and Eric F. Darve. Large-scale stochastic linear inversion using hierarchical matrices. *Computational Geosciences*, 17(6):913–927, 2013.
- [6] Sivaram Ambikasaran, Arvind K. Saibaba, Eric F. Darve, and Peter K. Kitanidis. Fast algorithms for Bayesian inversion. In *Computational Challenges in the Geosciences*, pages 101–142. Springer, 2013.
- [7] Sivaram Ambikasaran, Daniel Foreman-Mackey, Leslie F. Greengard, David W. Hogg, and Michael

- O'Neil. Fast direct methods for Gaussian processes and the analysis of NASA Kepler mission data. *arXiv preprint arXiv:1403.6015*, 2014.
- [8] Amirhossein Aminfar, Sivaram Ambikasaran, and Eric F. Darve. A fast block low-rank dense solver with applications to finite-element matrices. *arXiv preprint arXiv:1403.5337*, 2014.
- [9] Walter E. Arnoldi. The principle of minimized iterations in the solution of the matrix eigenvalue problem. *Quart. Appl. Math.*, 9(1):17–29, 1951.
- [10] Josh Barnes and Piet Hut. A hierarchical  $\mathcal{O}(N \log N)$  force-calculation algorithm. *Nature*, 324(4):446–449, 1986.
- [11] Rick K. Beatson and Leslie F. Greengard. A short course on fast multipole methods. *Wavelets, multilevel methods and elliptic PDEs*, pages 1–37, 1997.
- [12] Rick K. Beatson and Garry N. Newsam. Fast evaluation of radial basis functions: I. *Computers & Mathematics with Applications*, 24(12):7–19, 1992.
- [13] Rick K. Beatson, Jon B. Cherrie, and Cameron T. Mouat. Fast fitting of radial basis functions: Methods based on preconditioned GMRES iteration. *Advances in Computational Mathematics*, 11(2):253–270, 1999.
- [14] Stephen D. Billings, Rick K. Beatson, and Garry N. Newsam. Interpolation of geophysical data using continuous global surfaces. *Geophysics*, 67(6):1810, 2002.
- [15] Steffen Börm.  $\mathcal{H}^2$ -matrix arithmetics in linear complexity. *Computing*, 77(1):1–28, 2006.
- [16] Steffen Börm. Efficient numerical methods for non-local operators:  $\mathcal{H}^2$ -matrix compression, algorithms and analysis. *European Mathematical Society*, 14, 2010.
- [17] Steffen Börm, Lars Grasedyck, and Wolfgang Hackbusch. Introduction to hierarchical matrices with applications. *Engineering Analysis with Boundary Elements*, 27(5):405–422, 2003.
- [18] Martin D. Buhmann. *Radial basis functions: theory and implementations*, volume 12. Cambridge University Press, 2003.
- [19] J.C. Carr, Rick K. Beatson, Jon B. Cherrie, T.J. Mitchell, W.R. Fright, B.C. McCallum, and T.R. Evans. Reconstruction and representation of 3D objects with radial basis functions. In *Proceedings of the 28th annual conference on Computer graphics and interactive techniques*, pages 67–76. ACM, 2001.
- [20] Shivkumar Chandrasekaran, Patrick Dewilde, Ming Gu, Timothy P Pals, and AJ van der Veen. *Fast stable solver for sequentially semi-separable linear systems of equations*. Springer, 2002.
- [21] Shivkumar Chandrasekaran, Patrick Dewilde, Ming Gu, William Lyons, and Timothy P Pals. A fast solver for HSS representations via sparse matrices. *SIAM Journal on Matrix Analysis and Applications*, 29(1):67–81, 2006.
- [22] Shivkumar Chandrasekaran, Ming Gu, and Timothy P Pals. A fast ULV decomposition solver for hierarchically semi-separable representations. *SIAM Journal on Matrix Analysis and Applications*, 28(3):603–622, 2006.
- [23] H. Cheng, Leslie F. Greengard, and Vladimir Rokhlin. A fast adaptive multipole algorithm in three dimensions. *Journal of Computational Physics*, 155(2):468–498, 1999.
- [24] Ronald R. Coifman, Vladimir Rokhlin, and S. Wandzura. The fast multipole method for the wave equation: A pedestrian prescription. *Antennas and Propagation Magazine, IEEE*, 35(3):7–12, 1993.
- [25] Eric F. Darve. The fast multipole method: numerical implementation. *Journal of Computational Physics*, 160(1):195–240, 2000.
- [26] Eric F. Darve. The fast multipole method I: Error analysis and asymptotic complexity. *SIAM Journal on Numerical Analysis*, 38(1):98–128, 2000.
- [27] A. De Boer, MS Van der Schoot, and H. Bijl. Mesh deformation based on radial basis function interpolation. *Computers & Structures*, 85(11-14):784–795, 2007.
- [28] William Fong and Eric F. Darve. The black-box fast multipole method. *Journal of Computational Physics*, 228(23):8712–8725, 2009.
- [29] Roland W. Freund. A transpose-free quasi-minimal residual algorithm for non-hermitian linear systems. *SIAM Journal on Scientific Computing*, 14:470, 1993.
- [30] Roland W. Freund and Noël M. Nachtigal. QMR: a quasi-minimal residual method for non-hermitian linear systems. *Numerische Mathematik*, 60(1):315–339, 1991.
- [31] Lars Grasedyck and Wolfgang Hackbusch. Construction and arithmetics of  $\mathcal{H}$ -matrices. *Computing*, 70(4):295–334, 2003.
- [32] Leslie F. Greengard. *The rapid evaluation of potential fields in particle systems*, volume 1987. the MIT

- Press, 1988.
- [33] Leslie F. Greengard and Vladimir Rokhlin. A fast algorithm for particle simulations. *Journal of Computational Physics*, 73(2):325–348, 1987.
  - [34] Leslie F. Greengard and Vladimir Rokhlin. A new version of the fast multipole method for the Laplace equation in three dimensions. *Acta Numerica*, 6(1):229–269, 1997.
  - [35] Leslie F. Greengard, Denis Gueyffier, Per-Gunnar Martinsson, and Vladimir Rokhlin. Fast direct solvers for integral equations in complex three-dimensional domains. *Acta Numerica*, 18(1):243–275, 2009.
  - [36] Nail A. Gumerov and Ramani Duraiswami. Fast radial basis function interpolation via preconditioned Krylov iteration. *SIAM Journal on Scientific Computing*, 29(5):1876–1899, 2007.
  - [37] Wolfgang Hackbusch. A sparse matrix arithmetic based on  $\mathcal{H}$ -matrices. Part I: Introduction to  $\mathcal{H}$ -matrices. *Computing*, 62(2):89–108, 1999.
  - [38] Wolfgang Hackbusch and Steffen Börm. Data-sparse approximation by adaptive  $\mathcal{H}^2$ -matrices. *Computing*, 69(1):1–35, 2002.
  - [39] Wolfgang Hackbusch and Steffen Börm.  $\mathcal{H}^2$ -matrix approximation of integral operators by interpolation. *Applied Numerical Mathematics*, 43(1):129–143, 2002.
  - [40] Wolfgang Hackbusch and Boris N Khoromskij. A sparse  $\mathcal{H}$ -matrix arithmetic. *Computing*, 64(1):21–47, 2000.
  - [41] Wolfgang Hackbusch and Boris N Khoromskij. A sparse  $\mathcal{H}$ -matrix arithmetic: general complexity estimates. *Journal of Computational and Applied Mathematics*, 125(1):479–501, 2000.
  - [42] Wolfgang Hackbusch and Z.P. Nowak. On the fast matrix multiplication in the boundary element method by panel clustering. *Numerische Mathematik*, 54(4):463–491, 1989.
  - [43] Wolfgang Hackbusch, Boris Khoromskij, and Stefan A Sauter. On  $\mathcal{H}^2$ -matrices. In Hans-Joachim Bungartz, Ronald H.W. Hoppe, and Christoph Zenger, editors, *Lectures on Applied Mathematics*, pages 9–29. Springer Berlin Heidelberg, 2000. ISBN 978-3-642-64094-0.
  - [44] Wolfgang Hackbusch, Lars Grasedyck, and Steffen Börm. *An introduction to hierarchical matrices*. Max-Planck-Inst. für Mathematik in den Naturwiss., 2001.
  - [45] William W. Hager. Updating the inverse of a matrix. *SIAM review*, pages 221–239, 1989.
  - [46] Magnus R. Hestenes and Eduard Stiefel. Methods of conjugate gradients for solving linear systems. *Journal of Research of the National Bureau of Standards*, 49(6):409–436, 1952.
  - [47] Kenneth L. Ho and Leslie F. Greengard. A fast direct solver for structured linear systems by recursive skeletonization. *SIAM Journal on Scientific Computing*, 34(5):2507–2532, 2012.
  - [48] Wai Yip Kong, James Bremer, and Vladimir Rokhlin. An adaptive fast direct solver for boundary integral equations in two dimensions. *Applied and Computational Harmonic Analysis*, 31(3):346–369, 2011.
  - [49] Jun Lai, Sivaram Ambikasaran, and Leslie F. Greengard. A fast direct solver for high frequency scattering from a large cavity in two dimensions. *arXiv preprint arXiv:1404.3451*, 2014.
  - [50] Jonghyun Lee, Sivaram Ambikasaran, Peter K. Kitanidis, Tissa H. Illangasekare, and Kathleen M. Smits. Hydrogeophysical data assimilation using a fast Kalman filter for managed aquifer recharge and recovery. In *AGU Fall Meeting Abstracts*, volume 1, page 1281, 2013.
  - [51] Judith Y. Li, Sivaram Ambikasaran, Eric F. Darve, and Peter K. Kitanidis. A Kalman filter powered by  $\mathcal{H}^2$ -matrices for quasi-continuous data assimilation problems. *Water Resources Research*, 2014.
  - [52] Per-Gunnar Martinsson. A fast direct solver for a class of elliptic partial differential equations. *Journal of Scientific Computing*, 38(3):316–330, 2009.
  - [53] Per-Gunnar Martinsson and Vladimir Rokhlin. A fast direct solver for boundary integral equations in two dimensions. *Journal of Computational Physics*, 205(1):1–23, 2005.
  - [54] Naoshi Nishimura. Fast multipole accelerated boundary integral equation methods. *Applied Mechanics Reviews*, 55(4):299–324, 2002.
  - [55] Christopher C. Paige and Michael A. Saunders. Solution of sparse indefinite systems of linear equations. *SIAM Journal on Numerical Analysis*, 12(4):617–629, 1975.
  - [56] Timothy P Pals. *Multipole for scattering computations: Spectral discretization, stabilization, fast solvers*. PhD thesis, University of California Santa Barbara, 2004.
  - [57] Sergej Rjasanow. Adaptive cross approximation of dense matrices. *IABEM 2002, International Association for Boundary Element Methods*, 2002.
  - [58] Yousef Saad and Martin H. Schultz. GMRES: A generalized minimal residual algorithm for solving

- nonsymmetric linear systems. *SIAM Journal on Scientific and Statistical Computing*, 7(3):856–869, 1986.
- [59] Arvind K. Saibaba, Sivaram Ambikasaran, Judith Y. Li, Peter K. Kitanidis, and Eric F. Darve. Application of hierarchical matrices to linear inverse problems in geostatistics. *Oil and Gas Science and Technology-Revue de l'IFP-Institut Francais du Petrole*, 67(5):857, 2012.
- [60] Robert Schaback. Creating surfaces from scattered data using radial basis functions. In *Mathematical Methods for Curves and Surfaces*, pages 477–496. University Press, 1995.
- [61] Henk A Van der Vorst. Bi-CGSTAB: A fast and smoothly converging variant of bi-CG for the solution of non-symmetric linear systems. *SIAM Journal on scientific and Statistical Computing*, 13(2):631–644, 1992.
- [62] J. G. Wang and G. R. Liu. A point interpolation mesh-less method based on radial basis functions. *International Journal for Numerical Methods in Engineering*, 54(11):1623–1648, 2002.
- [63] Max A Woodbury. Inverting modified matrices. Statistical Research Group, Memo. Rep. no. 42, Princeton University, 1950.
- [64] Zong-min Wu and Robert Schaback. Local error estimates for radial basis function interpolation of scattered data. *IMA Journal of Numerical Analysis*, 13(1):13–27, 1993.
- [65] Lexing Ying, George Biros, and Denis Zorin. A kernel-independent adaptive fast multipole algorithm in two and three dimensions. *Journal of Computational Physics*, 196(2):591–626, 2004.
- [66] Kezhong Zhao, Marinos N Vouvakis, and J-F Lee. The adaptive cross approximation algorithm for accelerated method of moments computations of EMC problems. *Electromagnetic Compatibility, IEEE Transactions on*, 47(4):763–773, 2005.